
META-LEARNING TO CALIBRATE GAUSSIAN PROCESSES WITH DEEP KERNELS FOR REGRESSION UNCERTAINTY ESTIMATION

A PREPRINT

Tomoharu Iwata

NTT Communication Science Laboratories, NTT Corporation

Atsutoshi Kumagai

NTT Computer and Data Science Laboratories, NTT Corporation

ABSTRACT

Although Gaussian processes (GPs) with deep kernels have been successfully used for meta-learning in regression tasks, its uncertainty estimation performance can be poor. We propose a meta-learning method for calibrating deep kernel GPs for improving regression uncertainty estimation performance with a limited number of training data. The proposed method meta-learns how to calibrate uncertainty using data from various tasks by minimizing the test expected calibration error, and uses the knowledge for unseen tasks. We design our model such that the adaptation and calibration for each task can be performed without iterative procedures, which enables effective meta-learning. In particular, a task-specific uncalibrated output distribution is modeled by a GP with a task-shared encoder network, and it is transformed to a calibrated one using a cumulative density function of a task-specific Gaussian mixture model (GMM). By integrating the GP and GMM into our neural network-based model, we can meta-learn model parameters in an end-to-end fashion. Our experiments demonstrate that the proposed method improves uncertainty estimation performance while keeping high regression performance compared with the existing methods using real-world datasets in few-shot settings.

1 Introduction

Estimating the uncertainty of a prediction in regression tasks is important for machine learning systems. When the confidence in a prediction is low, decision-making can be passed on human experts to improve reliability [30, 4, 41]. Accurate uncertainty estimation is also beneficial for Bayesian optimization [55], reinforcement learning [68, 39, 20, 9], and active learning [19]. Many machine learning models, such as neural networks and Gaussian processes (GP) [49], achieve high accuracy but have no uncertainty estimates or poorly calibrated [24, 63, 40]. To estimate uncertainty, several approaches have been proposed [1, 59, 52]. For example, calibration methods transform the output of a trained prediction model using a non-decreasing function such that the predicted and empirical probabilities match. However, the existing methods require many data for training. In real-world applications, enough data can be unavailable in tasks of interest, and preparing sufficient data for each task requires high costs and is time-consuming.

We propose a meta-learning method for estimating uncertainty in regression tasks with a small amount of data. Meta-learning methods based on GPs with deep kernels [66] have been successfully used for improving the regression performance on unseen tasks with few data by learning to learn from various tasks [62, 16, 25, 46, 28]. However, these existing meta-learning methods are not designed for uncertainty estimation. The proposed method trains a regression model using data in multiple tasks such that the expected uncertainty estimation performance is improved when the model is adapted and calibrated to each task. Figure 1 illustrates our problem setting.

Our model consists of task-shared and task-specific components. With the task-shared components, we can share knowledge between tasks. With the task-specific components, we can handle the heterogeneity of tasks. Our meta-learning framework is formulated as a bilevel optimization, where the inner optimization corresponds to the adaptation and calibration of the task-specific components, and the outer optimization corresponds to the estimation of the task-shared components. Since the inner optimization is repeated for each outer optimization epoch, an effective inner

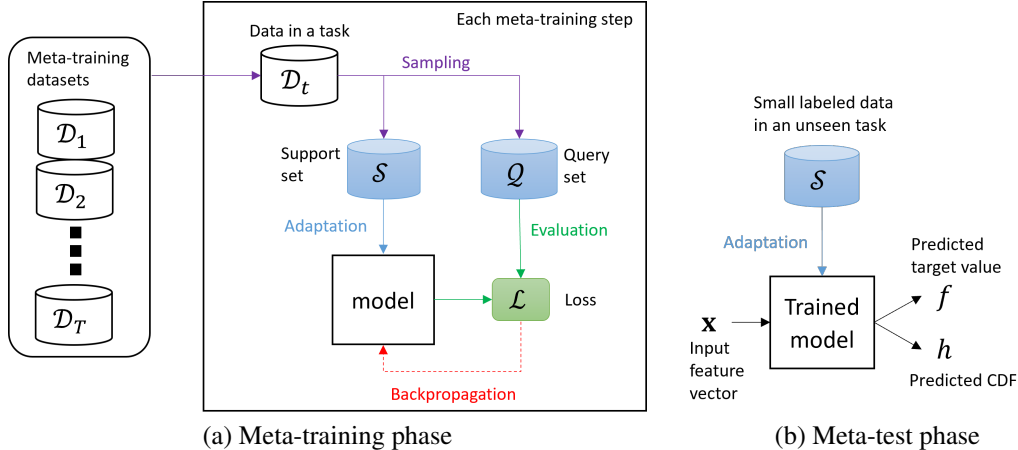


Figure 1: Problem setting. (a) In the meta-training phase, given meta-training datasets from various tasks, our model is meta-learned. For each step, support and query sets are randomly sampled from a randomly sampled dataset. The support set is used for adapting the model to the task. The query set is used to evaluate the model for minimizing the test prediction and calibration losses based on backpropagation. (b) In the meta-test phase, given a small number of labeled data \mathcal{S} in an unseen task, we predict target value f and its CDF h using the trained model adapted to \mathcal{S} .

optimization that allows backpropagation is essential. Although the adaptation and calibration are usually performed by iterative procedures based on gradient descent [35], backpropagation through such procedures is costly in terms of memory, and the total number of iterations must be kept small [15]. On the other hand, we design our regression model such that the inner optimization is performed without iterative procedures.

In our model, an uncalibrated output distribution is modeled by a GP with a task-shared encoder network. With the GP, the task-adapted output distribution can be obtained in a closed form. Since the uncertainty estimation performance of the output distribution can be low, we calibrate it using a cumulative density function (CDF) of a task-specific Gaussian mixture model (GMM), which is a non-decreasing and differentiable function, such that the output distribution matches the empirical one. The parameters of the GMM can be determined without iterative procedures. In the outer optimization, the task-shared parameters are estimated by minimizing the test expected calibration and regression errors using a stochastic gradient descent method with an episodic training framework [50]. Since the adaptation and calibration of our model are differentiable, we can backpropagate the losses through them to update the task-shared components in an end-to-end manner.

The main contributions of this paper are as follows: 1) We propose a meta-learning method for regression uncertainty estimation that directly minimizes the test expected calibration error. 2) We develop differentiable adaptation and calibration functions that do not require iterative optimization procedures. 3) We empirically demonstrate that the proposed method outperforms the existing uncertainty estimation methods.

2 Related work

Many methods for regression uncertainty estimation have been proposed. Calibration methods map an output of a pretrained model to a calibrated one [48, 35, 65, 44, 10, 40]. Quantile regression estimates quantiles of the output distribution, often by the pinball loss [14, 53, 60, 47, 29]. Some methods use models that output density function estimates [69, 56, 37, 38, 27, 7, 17, 34]. We employed the calibration approach since it has been used in a wide variety of applications, and it enables us to design a model that can perform the adaptation and calibration without iterative procedures. The existing calibration methods use calibration models that require iterative optimization procedures [12], such as isotonic regression [35], or that are not differentiable [40]. In contrast, our calibration model is differentiable and obtained without iterative procedures, and therefore, we can perform meta-learning effectively.

Most existing meta-learning methods are developed to improve regression or classification performance [54, 5, 15, 64, 57], but not uncertainty estimation performance. There are some meta-learning methods for estimating classification uncertainty [8, 67, 32], but not for regression uncertainty. Neural processes [22, 21, 31, 43] are a meta-learning approach for few-shot regression with uncertainty estimation. Since their prediction is based on fully parametric models, they are less flexible in adapting to the given data [28]. Functional PAC-optimal hyper-posterior (F-PACOH) [51] is a meta-learning method to improve uncertainty estimation by alleviating meta-overfitting in the case of few meta-training

tasks by regularizing priors in the function space. F-PACOH is not a calibration method, and it can be combined with the proposed method to directly minimize the test expected calibration error. Although [8] proposed a differentiable expected calibration error for classification tasks, it is inapplicable to regression tasks. In meta-learning, models that can adapt to each task without iterative procedures have been successfully used for classification and regression tasks using linear or GP regression models [6, 28, 46]. However, they do not consider uncertainty calibration. In addition, unlike these existing methods, the proposed method achieves non-iterative task adaptation for a two-step method, i.e., regression by GP and its calibration by non-decreasing function, by properly connecting differentiable approaches for regression and calibration.

3 Preliminaries: Calibration

Let $h(y|\mathbf{x}) : \mathcal{Y} \times \mathcal{X} \rightarrow [0, 1]$ be the cumulative distribution function (CDF) of target value $y \in \mathcal{Y} \subseteq \mathbb{R}$ at input feature vector $\mathbf{x} \in \mathcal{X}$. We can quantify the uncertainty of the prediction by the CDF, which is the probability that the target value is less than y given input \mathbf{x} . The inverse function of the CDF $h^{-1}(p|\mathbf{x}) : [0, 1] \times \mathcal{X} \rightarrow \mathcal{Y}$ is used to denote the quantile function. The CDF is well calibrated when it matches with the empirical CDF as sample size N goes to infinity [13, 35]:

$$\frac{1}{N} \sum_{n=1}^N I(y_n \leq h^{-1}(p|\mathbf{x}_n)) \rightarrow p, \quad (1)$$

as $N \rightarrow \infty$ for all $p \in [0, 1]$.

Given data $\{(\mathbf{x}_n, y_n)\}_{n=1}^N$, uncalibrated CDF $h_U(y|\mathbf{x})$ is calibrated by non-decreasing function $r : [0, 1] \rightarrow [0, 1]$, where $r(p_{(1)}), \dots, r(p_{(N)})$ are evenly spaced on the unit interval, and $p_{(n)} = h_U(y_{(n)}|\mathbf{x}_{(n)})$ is the n th smallest uncalibrated CDF in the given data. An example of such a non-decreasing function is the following empirical calibration model [40]:

$$r_{\text{emp}}(p) = \frac{n}{N} \quad \text{if } p \in [p_{(n)}, p_{(n+1)}), \quad (2)$$

where $\frac{n}{N}$ is the empirical CDF between $p_{(n)}$ and $p_{(n+1)}$. Figure 3(a) shows an example of r_{emp} . Although the empirical calibration model can calibrate uncertainty on given data, its generalization performance for uncertainty estimation can be poor, especially when only a small number of data are given. A calibrated CDF is given by $h(y|\mathbf{x}) = r(h_U(y|\mathbf{x}))$ using uncalibrated model h_U and calibration model r .

4 Proposed method

In Section 4.1, we present our problem formulation tackled in this paper. In Section 4.2, we propose our model that outputs task-specific calibrated CDF h given a small number of data. In Section 4.3, we present meta-learning procedures for our model that improve uncertainty estimation performance.

4.1 Problem formulation

In the meta-training phase, we are given meta-training datasets $\{\mathcal{D}_t\}_{t=1}^T$ from T tasks, where $\mathcal{D}_t = \{(\mathbf{x}_{tn}, y_{tn})\}_{n=1}^{N_t}$ is the dataset of the t th task, $\mathbf{x}_{tn} \in \mathcal{X}$ is the n th feature vector, $y_{tn} \in \mathbb{R}$ is its target value, and N_t is the number of instances. In the meta-test phase, we are given a small number of labeled instances $\mathcal{S} = \{(\mathbf{x}_n^S, y_n^S)\}_{n=1}^{N^S}$, which is called the support set, from an unseen meta-test task that is different from the meta-training tasks. We are also given unlabeled instances, which are called the query set, from the meta-test task. Our aim is to improve the test uncertainty estimation performance and test regression performance on the query set in such meta-test tasks.

4.2 Model

We design our model to output predicted target value f and calibrated CDF h such that it can be adapted to support set \mathcal{S} without iterative optimization. An uncalibrated CDF is modeled by the GP with deep kernels as described in Section 4.2.1, and its calibration is presented in Section 4.2.2. Figure 2 illustrates our model.

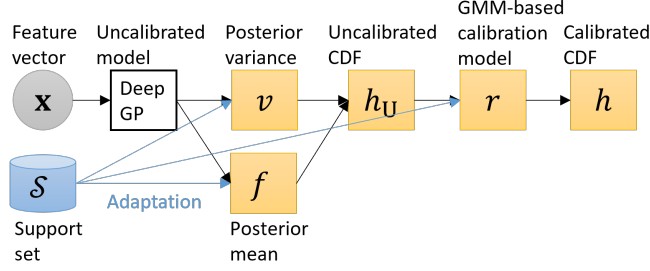


Figure 2: Proposed model. The task-shared/task-specific components in the proposed model are represented by white/yellow boxes, and the forwarding procedure is represented by black arrows. Posterior mean f and variance v are modeled by GP with deep kernels, or deep GP. Uncalibrated CDF h_U is calculated from them. Calibrated CDF h is obtained by transforming uncalibrated CDF h_U by GMM-based calibration model r . Posterior mean f , posterior variance v , and calibration model r are adapted for each task using support set \mathcal{S} as represented by blue arrows.

4.2.1 Uncalibrated model

We model an uncalibrated CDF using GP with deep kernels [66], $\text{GP}(\mu(\mathbf{x}), k(\mathbf{x}, \mathbf{x}'))$. Here, μ is the mean function based on a feed-forward neural network, and k is the following Gaussian kernel with an additive noise term,

$$k(\mathbf{x}, \mathbf{x}') = \exp\left(-\frac{1}{2} \|\mathbf{g}(\mathbf{x}) - \mathbf{g}(\mathbf{x}')\|^2\right) + \beta\delta(\mathbf{x}, \mathbf{x}'), \quad (3)$$

where \mathbf{g} is an encoder based on a feed-forward neural network, $\beta > 0$ is an observation's additive noise parameter, and $\delta(\mathbf{x}, \mathbf{x}')$ is the Kronecker delta function, $\delta(\mathbf{x}, \mathbf{x}') = 1$ if \mathbf{x} and \mathbf{x}' are identical, and zero otherwise. Neural networks, μ and \mathbf{g} , and kernel parameter β are shared across tasks, by which we can accumulate knowledge that is useful for uncertainty estimation in different tasks in model parameters, and use it for unseen tasks. With neural network \mathbf{g} , we can flexibly encode input features such that the target value is accurately predicted by the GP in the encoded space. With the GP, the posterior probability density distribution of the target value adapted to support set \mathcal{S} is calculated in a closed form by the following Gaussian,

$$p_U(y|\mathbf{x}; \mathcal{S}) = \mathcal{N}(y|f(\mathbf{x}; \mathcal{S}), v(\mathbf{x}; \mathcal{S})), \quad (4)$$

where

$$f(\mathbf{x}; \mathcal{S}) = \mu(\mathbf{x}) + \mathbf{k}^\top \mathbf{K}^{-1}(\mathbf{y}^{\mathcal{S}} - \mathbf{m}), \quad v(\mathbf{x}; \mathcal{S}) = k(\mathbf{x}, \mathbf{x}) - \mathbf{k}^\top \mathbf{K}^{-1} \mathbf{k}, \quad (5)$$

are its mean and variance, $\mathbf{y}^{\mathcal{S}} = (y_n^{\mathcal{S}})_{n=1}^{N^{\mathcal{S}}} \in \mathbb{R}^{N^{\mathcal{S}}}$ is the target vector of the support instances, $\mathbf{K} \in \mathbb{R}^{N^{\mathcal{S}} \times N^{\mathcal{S}}}$ is the matrix of the kernel function evaluated among the support instances, $\mathbf{K}_{nn'} = k(\mathbf{x}_n^{\mathcal{S}}, \mathbf{x}_{n'}^{\mathcal{S}})$, $\mathbf{k} = (k(\mathbf{x}, \mathbf{x}_n^{\mathcal{S}}))_{n=1}^{N^{\mathcal{S}}} \in \mathbb{R}^{N^{\mathcal{S}}}$ is the vector of the kernel function evaluated between \mathbf{x} and the support instances, $\mathbf{m} = (\mu(\mathbf{x}_n^{\mathcal{S}}))_{n=1}^{N^{\mathcal{S}}} \in \mathbb{R}^{N^{\mathcal{S}}}$ is the vector of the mean function evaluated on the support instances, and $\mathcal{N}(\cdot|\mu, \sigma^2)$ is the Gaussian probability distribution function with mean μ and variance σ^2 . Posterior mean $f(\mathbf{x}; \mathcal{S})$ corresponds to the predicted target value. Using Eq. (4), the uncalibrated CDF is given by

$$h_U(y|\mathbf{x}; \mathcal{S}) = \int_{-\infty}^y p_U(y'|\mathbf{x}; \mathcal{S}) dy' = \frac{1}{2} \left(1 + \text{erf} \left(\frac{y - f(\mathbf{x}; \mathcal{S})}{\sqrt{2v(\mathbf{x}; \mathcal{S})}} \right) \right), \quad (6)$$

which can be calculated using error function $\text{erf}(y) = \frac{2}{\sqrt{\pi}} \int_0^y \exp(-y'^2) dy'$. The gradient of the error function, which is required for backpropagation, follows immediately from its definition $\frac{\partial \text{erf}(y)}{\partial y} = \frac{2}{\sqrt{\pi}} \exp(-y^2)$, which is given in a closed form.

4.2.2 Calibration model

We calibrate uncalibrated CDF h_U using a task-specific non-decreasing function, for which we use the CDF of the following Gaussian mixture model,

$$q(h'; \mathcal{S}) = \frac{1}{N^{\mathcal{S}}} \sum_{(\mathbf{x}^{\mathcal{S}}, y^{\mathcal{S}}) \in \mathcal{S}} \mathcal{N}(h'|h_U(y^{\mathcal{S}}|\mathbf{x}^{\mathcal{S}}; \mathcal{S}), \sigma^2), \quad (7)$$

where the number of components is the number of support instances N^S , the mean of each component is the uncalibrated CDF in Eq. (6) at each support instance, variance σ^2 is a task-shared parameter to be trained, and the mixture weight is $\frac{1}{N^S}$. Its CDF is given by

$$r(h'; \mathcal{S}) = \int_{-\infty}^{h'} q(h''; \mathcal{S}) dh'' = \frac{1}{2N^S} \sum_{(\mathbf{x}^S, y^S) \in \mathcal{S}} \left(1 + \operatorname{erf} \left(\frac{h' - h_U(y^S | \mathbf{x}^S; \mathcal{S})}{\sqrt{2}\sigma} \right) \right), \quad (8)$$

where it is a non-decreasing function. As variance σ^2 goes to zero, our calibration model in Eq. (8) gets close to the empirical calibration model in Eq. (2). Although the empirical calibration model is not differentiable, our calibration model is differentiable. By using the Gaussian mixture model, we can obtain a differentiable non-decreasing function for calibration without iterative optimization. An example of calibration model r is shown in Figure 3(b). It is smooth and non-decreasing, and its slope is steep where the support instances exist. Although uncalibrated model $h_U(y|\mathbf{x})$ in Eq. (6) can model only a Gaussian distribution, calibrated model $r(h(y|\mathbf{x}))$ using Eq. (8) can model a non-Gaussian distribution.

The existing calibration methods usually prepare data for calibration that are different from data for training an uncalibrated prediction model to avoid overfitting [35]. However, since we consider a situation where the number of support instances is small, splitting them into two can be unprofitable. Therefore, we use support set \mathcal{S} for adapting both uncalibrated and calibration models. Since we train task-shared parameters such that the test calibration loss is minimized as described in the next subsection, we can alleviate the overfitting of the calibration. To additionally reduce the risk of overfitting, we use the following mixture of calibrated and uncalibrated CDFs,

$$h(y|\mathbf{x}, \mathcal{S}) = \alpha h_U(y|\mathbf{x}; \mathcal{S}) + (1 - \alpha)r(h_U(y|\mathbf{x}; \mathcal{S}); \mathcal{S}), \quad (9)$$

where $\alpha \in [0, 1]$ is a task-shared weight parameter that can be trained automatically using meta-training datasets. When $r(p)$ is a non-increasing function, $\alpha p + (1 - \alpha)r(p)$ is also a non-increasing function.

Figures 3(c,d) show the predicted target values and their uncertainty with our uncalibrated and calibrated models. In both models, the uncertainty was small, and the predicted target values were close to true ones around the support instances, and the uncertainty was large where the support instances were located far away. These results are reasonable. However, the uncertainty by the uncalibrated model was generally large, and poorly calibrated. By the calibration, the uncertainty was tightened while most of the true target values were within the 95% confidence interval, and well-calibrated. Since the uncalibrated model can model only a Gaussian distribution, the confidence interval was always symmetrical around the predicted target values. On the other hand, the calibrated model can represent an unsymmetric confidence interval.

Figure 4 shows the relationship between the estimated and empirical CDFs when calibrated with empirical calibration model r_{emp} in Eq. (2) and with our calibration model. When the estimated and empirical CDFs match as shown in the black line, it is perfectly calibrated. The calibration of the empirical CDF on the support instances is easily achievable via the empirical calibration model as shown in (a). However, its estimated CDF on the query instances was poorly calibrated due to overfitting, which is undesirable since our aim is to improve the test uncertainty estimation performance. On the other hand, the estimated CDF on the query instances by our calibrated model was closer to the empirical CDF than that by the uncalibrated model and that by the empirical calibration model.

4.3 Meta-learning

The parameters ϕ shared across tasks in our model are parameters in encoder network g in Eq. (3), parameters in neural network-based mean function μ in Eq. (5), kernel parameter β in Eq. (3), variance σ^2 in the calibration model in Eq. (7), and weight α in the calibrated CDF in Eq. (9). We train ϕ such that the test target prediction performance and test uncertainty estimation performance are improved. Let \mathcal{Q} be the query set, which contains held-out data different from support set \mathcal{S} in a task. For evaluating the test target prediction performance of prediction model f on the meta-training tasks, we use the following regression loss, $\mathcal{L}_R(f, \mathcal{Q}) = \frac{1}{N^Q} \sum_{(\mathbf{x}, y) \in \mathcal{Q}} \|f(\mathbf{x}) - y\|^2$, which is the mean squared error between true and predicted target values over the query instances. For evaluating the test uncertainty estimation performance of CDF h , we use the following calibration loss,

$$\mathcal{L}_C(h, \mathcal{Q}) = \frac{1}{N^Q} \sum_{n=1}^{N^Q} \left| p_{(n)} - \frac{n}{N^Q} \right|, \quad (10)$$

where $p_{(n)}$ is the n th smallest CDF estimated by h in the query instances, and $\frac{n}{N^Q}$ is the empirical CDF of the query instances at $p_{(n)}$. When the calibration loss is small, the empirical and estimated CDFs are close. For the total loss, we use the following weighted average of the regression and calibration losses,

$$\mathcal{L}(f, h, \mathcal{Q}) = \lambda \mathcal{L}_R(f, \mathcal{Q}) + (1 - \lambda) \mathcal{L}_C(h, \mathcal{Q}), \quad (11)$$

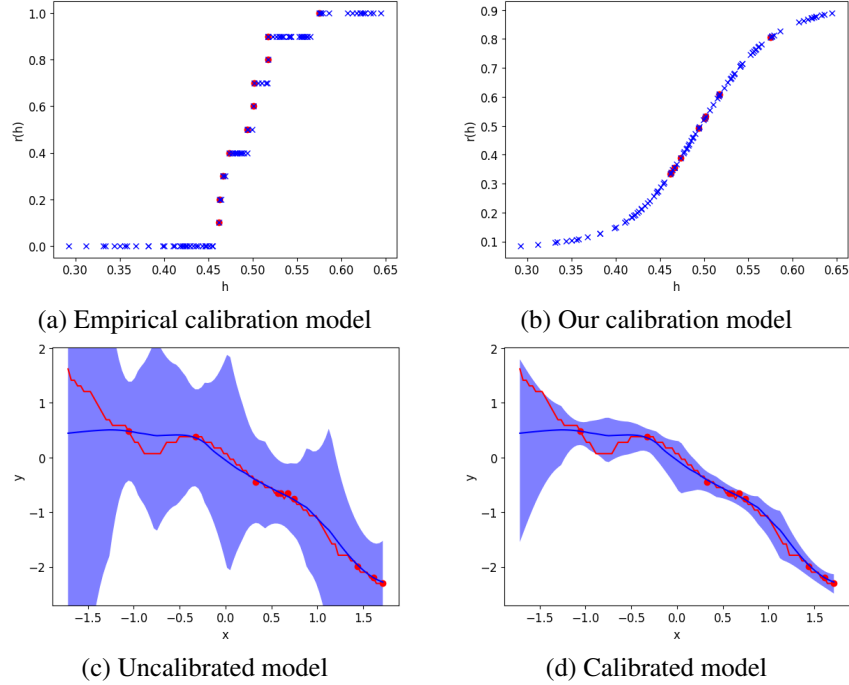


Figure 3: (a) Empirical calibration model. The horizontal axis is the uncalibrated CDF, and the vertical axis is its calibrated one with the calibration model r_{emp} in Eq. (2). A red point shows a support instance, and a blue point shows a query instance. Here, we used the AHM dataset (see Section 5 for details, and we also used the same data in (b,c) and Figure 4). (b) Our calibration model r in Eq. (8). (c) Our uncalibrated model adapted to a support set, and (d) its calibrated one with our calibration model. The horizontal axis is the input feature value, and the vertical axis is the target value. A red point shows a support instance, a red line shows true target values, a blue line shows predicted target values, and a blue area shows estimated 95% confidence intervals. Here, we used the AHM dataset (see Section 5 for details, and we also used the same data in (b,c) and Figure 4).

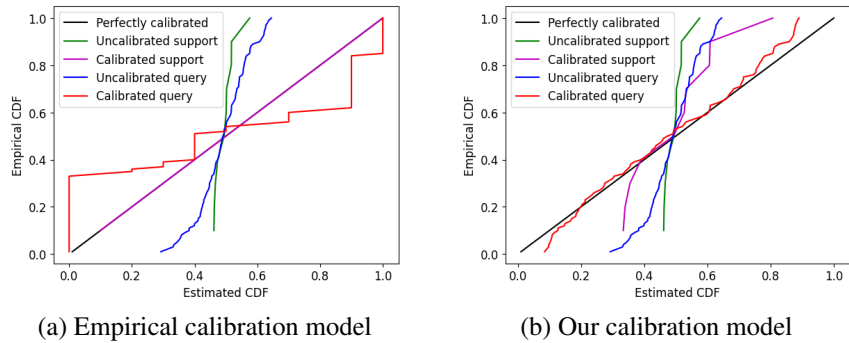


Figure 4: Estimated CDFs of uncalibrated/calibrated models and empirical CDFs on support/query instances by empirical calibration model r_{emp} in Eq. (2) (a) and by our calibration model (b). The black line shows the perfectly calibrated estimated CDF and the empirical CDF. The green/purple line shows the estimated uncalibrated CDF and the empirical CDF on support/query instances. The blue/red line shows the estimated calibrated CDF and the empirical CDF on support/query instances.

where $0 \leq \lambda \leq 1$ is a hyperparameter that can be determined depending on its application. In our experiments, the performance was not sensitive to λ unless λ was almost zero or one. Although proper scoring rules [23], such as the negative log-likelihood and pinball loss [29], can consider both regression and calibration performance in a measurement indirectly, they fail to minimize calibration error because of overfitting [36]. Therefore, we directly use the regression and calibration errors for the objective function in Eq. (11) as in [36].

Algorithm 1 Meta-learning procedures of our model.

Input: Meta-training data $\{\mathcal{D}\}_{t=1}^T$, support set size N^S , query set size N^Q .

Output: Trained task-shared parameters ϕ .

- 1: **while** End condition is not satisfied **do**
 - 2: Randomly select task index t from $\{1, \dots, T\}$.
 - 3: Randomly sample N^S instances from \mathcal{D}_t for support set \mathcal{S} .
 - 4: Randomly sample N^Q instances from $\mathcal{D}_t \setminus \mathcal{S}$ for query set \mathcal{Q} .
 - 5: Calculate uncalibrated PDF p_U adapted to support set \mathcal{S} by Eq. (4).
 - 6: Calculate uncalibrated CDF h_U by Eq. (6).
 - 7: Calculate calibration model r adapted to support set \mathcal{S} by Eq. (8).
 - 8: Calculate calibrated CDF h by Eq. (9).
 - 9: Calculate loss \mathcal{L} on query set \mathcal{Q} by Eq. (11).
 - 10: Update model parameters ϕ using the gradient of the loss by a stochastic gradient method.
 - 11: **end while**
-

We estimate parameters ϕ by minimizing the following expected total loss calculated using meta-training datasets $\{\mathcal{D}_t\}_{t=1}^T$,

$$\hat{\phi} = \arg \min_{\phi} \mathbb{E}_t \mathbb{E}_{\mathcal{S}, \mathcal{Q} \sim \mathcal{D}_t} [\mathcal{L}(f(\cdot; \mathcal{S}), h(\cdot; \mathcal{S}), \mathcal{Q})], \quad (12)$$

where \mathbb{E}_t is the expectation over meta-training tasks, $\mathbb{E}_{\mathcal{S}, \mathcal{Q} \sim \mathcal{D}_t}$ is the expectation over support and query sets that are randomly generated without overlap from a meta-training dataset \mathcal{D}_t , $f(\cdot; \mathcal{S})$ is the target prediction model adapted to support set \mathcal{S} in Eq. (5), and $h(\cdot; \mathcal{S})$ is the calibrated CDF adapted to support set \mathcal{S} in Eq. (9). We can improve the test performance by Eq. (12) since the support set for adaptation and calibration is different from the query set for evaluation. When the task distribution in meta-training data is the same as that in meta-test data, Eq. (12) improves the generalization performance for the meta-test data. Since both models f and h are differentiable, we can minimize it using a stochastic gradient descent method [33]. Algorithm 1 shows the meta-learning procedures of our model. The expectation in Eq. (12) is approximated by the Monte Carlo method by randomly sampling tasks, support, and query sets from the meta-training datasets in Lines 2–4. The time complexity cubically increases with the number of support instances N^S due to the inverse in Eqs. (5). Since we consider situations where the number of support instances is small, our model can be optimized efficiently.

5 Experiments

5.1 Data

To evaluate the proposed method, we used the following five data sets: AHM, MAT, School, Tafeng, and Sales. AHM and MAT are the spatial data of the annual heat-moisture index and mean annual temperature in North America. School is a benchmark dataset in multi-task regression [3, 2], which contains the examination scores of students from different schools (tasks). Sales and Tafeng contain weekly purchased quantities of products [26].

AHM and MAT were the spatial data of the annual heat-moisture index and mean annual temperature in North America, which were obtained from <https://sites.ualberta.ca/~ahamann/data/climatena.html>. We used 365 non-overlapping regions (tasks), where the size of each region was 100×100 km, and the target values were observed at 1×1 km grid squares in each region. The number of features in AHM was one (longitude), and the number of features in MAT was three (longitude, latitude, and elevation). School is a benchmark dataset in multi-task regression [3, 2], which contains the examination scores of students from 139 schools (tasks). We used schools with 60 or more students, ending up with 109 tasks. The number of features was 28, and the average number of instances per task was 129. Sales contains weekly purchased quantities of 811 products over 52 weeks [61]. We obtained the dataset from the UCI repository. Following [26], we used the sales of five previous weeks for each product as features, and the sales for the current week (task) as targets. The number of features was five, the number of tasks was 47, and the number of instances per task was 811. Tafeng is another grocery shopping dataset that contains transactions of 23,812 products over four months. We build the data in a similar fashion to Sales. The number of features was five, the number of tasks was 13, and the number of instances per task was 23,812.

For each dataset, we randomly split the tasks, where 60% of them were used for meta-training, 20% for meta-validation, and the remaining for meta-test.

5.2 Compared methods

We compared the proposed method (Ours) with the following methods: meta-learning with deep kernel learning (MDKL) [28], neural process (NP) [21], simultaneous quantile regression (SQR) [60], neural network-based Gaussian model (NG), Bayesian dropout (BD) [18], Gaussian process (GP), and meta-learning versions of SQR, NG, and BD (MSQR, MNG, and MBD) based on model-agnostic meta-learning (MAML) [15]. SQR, NG, BD, and GP are single-task methods, which train models for each task. MDKL, NP, MSQR, MNG, MBD, and Ours are meta-learning methods, which train task-shared neural networks using meta-training datasets.

With MDKL, the GP with deep kernels is used, where the neural network and kernel parameters are trained by maximizing the expected test likelihood on query sets. NP is a neural network-based meta-learning method, where a task representation is encoded using the support set, and the predictive mean and variance are calculated using the task representation. With MDKL, the GP with deep kernels is used. In NP and MDKL, the model parameters are trained by maximizing the expected test likelihood on query sets. SQR is a neural network model that outputs a quantile target value given a feature vector and quantile level, which is trained by minimizing the pinball loss for various quantile levels $p \in [0.1, 0.2, \dots, 0.9]$. NG is a neural network model that outputs the predictive mean and variance of a Gaussian distribution of a target value given a feature vector, which is trained by maximizing the likelihood. With BD, a neural network regression model is trained by minimizing the mean squared error with dropout, and the mean and variance of a target value are estimated by sampling multiple target values with dropout. The dropout rate was 0.3, and the number of samples was 30. With GP, the RBF kernel was used, where the kernel parameters were trained by maximizing the expected test likelihood using meta-training datasets. With MAML-based methods, the task adaptation was performed by the gradient descent method with learning rate 10^{-2} and five epochs.

5.3 Settings

For encoder network g in the proposed method, MDKL, and NP, we used a three-layered feed-forward neural network with 32 hidden and output units. For mean function f in the proposed method and MDKL, and for neural networks in comparing methods, we used four-layered feed-forward neural networks with 32 hidden units. We optimized the models using Adam [33] with learning rate 10^{-2} , and a batch size of 32 tasks. The number of meta-training epochs was 1,000, and the meta-validation data were used for early stopping. We implemented the methods with PyTorch [45]. The number of support instances per task was $\{10, 20, 30\}$, and the number of query instances was 30.

5.4 Measurements

For the evaluation measurement of the target prediction and uncertainty estimation performance, we used the mean squared error (MSE) and expected calibration error (ECE) [42, 24] on query sets in the meta-test tasks. The MSE is calculated by the squared error between true and predicted targets, $\text{MSE} = \frac{1}{N^Q} \sum_{(\mathbf{x}, y) \in \mathcal{Q}} \|y - f(\mathbf{x})\|^2$. The ECE is a widely-used measurement for uncertainty estimation performance, which is calculated by the absolute error between quantile level p and empirical probability \hat{p} that the target value is below the quantile function, $\text{ECE} = \frac{1}{|\mathcal{P}|} \sum_{p \in \mathcal{P}} |p - \hat{p}(p, h, \mathcal{Q})|$, where $\hat{p}(p, h, \mathcal{Q}) = \frac{1}{N^Q} \sum_{(\mathbf{x}, y) \in \mathcal{Q}} I(y \leq h^{-1}(p|\mathbf{x}))$ and $\mathcal{P} = \{0.1, 0.2, \dots, 0.9\}$. For evaluating both performances simultaneously, we used the total error (TE), which is the average of the MSE and ECE, $\text{TE} = \frac{\text{MSE} + \text{ECE}}{2}$. We averaged the TE, MSE, and ECE over ten experiments with different splits of meta-training, validation, and test data.

5.5 Results

Tables 1, 2 and 3 show the test total error, MSE and ECE. The proposed method achieved the lowest test total error in all cases. As the number of support instances increased, the performance generally rose. MDKL corresponds to the proposed method without uncertainty calibration that minimizes the regression loss. Although the MSEs by the proposed method were close to those by MDKL, the ECEs by the proposed method were always better than those by MDKL. This result demonstrates the effectiveness of our calibration model and calibration loss. MAML-based meta-learning methods often improved the performance compared with their single-task versions. However, they failed to meta-learn well on the AHM dataset. Since MAML uses a small number of gradient descent steps for adaptation, the adaptation can be insufficient. In contrast, since the proposed method performs task adaptation and calibration without iterative procedures, its meta-learning becomes stable, resulting in its low errors. The MSEs by the proposed method and MDKL were generally lower than the other methods. This result indicates the efficacy of the GP-based closed-form solver for task adaptation in regression.

Figure 5 shows that the test total error decreased as the number of training tasks rose with the proposed method. This result indicates that the proposed method can meta-learn from various tasks, and use the knowledge for unseen tasks.

Table 1: Test total error, which is the average of MSE and ECE, with different numbers of support instances N^S . Values in bold typeface are not statistically significantly different at the 5% level from the best performing method in each row according to a paired t-test.

Data	N^S	Ours	MDKL	NP	MSQR	MNG	MBD	SQR	NG	BD	GP
AHM	10	0.167	0.184	0.262	0.809	0.857	0.870	0.532	0.564	0.248	0.202
AHM	20	0.097	0.120	0.229	0.796	0.850	0.858	0.517	0.556	0.195	0.127
AHM	30	0.077	0.104	0.214	0.789	0.840	0.846	0.504	0.541	0.186	0.107
MAT	10	0.123	0.133	0.124	0.272	0.382	0.325	0.540	0.431	0.222	0.134
MAT	20	0.094	0.106	0.114	0.271	0.383	0.325	0.526	0.415	0.171	0.107
MAT	30	0.077	0.095	0.112	0.276	0.380	0.328	0.525	0.410	0.155	0.096
School	10	0.383	0.381	0.381	0.392	0.415	0.478	0.662	0.581	0.756	0.382
School	20	0.380	0.379	0.377	0.383	0.410	0.477	0.645	0.552	0.683	0.379
School	30	0.373	0.371	0.375	0.377	0.404	0.466	0.632	0.533	0.616	0.373
Tafeng	10	0.957	0.928	1.036	0.910	1.129	0.984	1.190	1.302	1.115	0.910
Tafeng	20	0.882	0.994	1.091	0.802	1.051	0.976	1.156	1.249	1.140	0.967
Tafeng	30	0.134	0.186	0.196	0.141	0.250	0.238	0.202	0.284	0.338	0.216
Sales	10	0.081	0.100	0.082	0.086	0.275	0.124	0.411	0.381	0.195	0.102
Sales	20	0.081	0.094	0.082	0.085	0.267	0.124	0.397	0.340	0.153	0.097
Sales	30	0.082	0.093	0.083	0.087	0.272	0.121	0.395	0.331	0.148	0.098

 Table 2: Test mean squared error (MSE) with different numbers of support instances N^S . Values in bold typeface are not statistically significantly different at the 5% level from the best performing method in each row according to a paired t-test.

Data	N^S	Ours	MDKL	NP	MSQR	MNG	MBD	SQR	NG	BD	GP
AHM	10	0.223	0.229	0.399	1.413	1.500	1.407	0.792	0.962	0.360	0.265
AHM	20	0.104	0.101	0.340	1.391	1.488	1.383	0.767	0.952	0.264	0.115
AHM	30	0.069	0.064	0.315	1.378	1.470	1.363	0.745	0.924	0.250	0.069
MAT	10	0.140	0.142	0.162	0.454	0.654	0.467	0.831	0.738	0.315	0.146
MAT	20	0.097	0.095	0.143	0.452	0.656	0.466	0.809	0.715	0.236	0.099
MAT	30	0.073	0.073	0.139	0.463	0.653	0.472	0.807	0.710	0.211	0.079
School	10	0.706	0.702	0.702	0.723	0.770	0.753	1.072	1.079	1.307	0.703
School	20	0.700	0.697	0.695	0.707	0.760	0.753	1.038	1.030	1.174	0.698
School	30	0.688	0.683	0.692	0.699	0.752	0.729	1.014	0.999	1.044	0.690
Tafeng	10	1.819	1.672	1.909	1.707	2.012	1.788	2.178	2.365	2.040	1.635
Tafeng	20	1.667	1.803	2.011	1.489	1.861	1.771	2.128	2.258	2.090	1.747
Tafeng	30	0.187	0.189	0.209	0.168	0.266	0.299	0.223	0.327	0.490	0.250
Sales	10	0.089	0.090	0.089	0.091	0.338	0.130	0.557	0.572	0.258	0.098
Sales	20	0.086	0.085	0.081	0.085	0.322	0.128	0.530	0.489	0.189	0.093
Sales	30	0.087	0.087	0.085	0.088	0.330	0.121	0.529	0.474	0.180	0.095

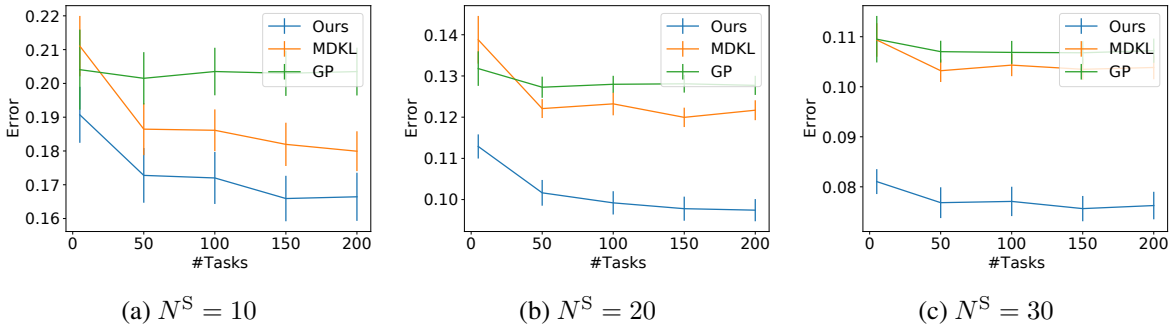


Figure 5: Test total error with different numbers of training tasks with the AHM datasets. The bar shows the standard error.

Table 3: Test expected calibration error (ECE) with different numbers of support instances N^S . Values in bold typeface are not statistically significantly different at the 5% level from the best performing method in each row according to a paired t-test.

Data	N^S	Ours	MDKL	NP	MSQR	MNG	MBD	SQR	NG	BD	GP
AHM	10	0.111	0.139	0.125	0.205	0.213	0.333	0.271	0.166	0.136	0.140
AHM	20	0.090	0.140	0.118	0.201	0.211	0.332	0.268	0.161	0.125	0.139
AHM	30	0.086	0.144	0.113	0.201	0.209	0.330	0.262	0.158	0.122	0.145
MAT	10	0.106	0.123	0.086	0.089	0.109	0.183	0.250	0.124	0.130	0.122
MAT	20	0.090	0.117	0.084	0.089	0.110	0.183	0.244	0.115	0.105	0.115
MAT	30	0.082	0.116	0.084	0.090	0.108	0.183	0.244	0.111	0.098	0.114
School	10	0.060	0.061	0.060	0.061	0.060	0.204	0.251	0.083	0.205	0.060
School	20	0.060	0.061	0.060	0.059	0.060	0.202	0.252	0.073	0.191	0.059
School	30	0.059	0.060	0.057	0.055	0.056	0.203	0.251	0.067	0.187	0.056
Tafeng	10	0.094	0.184	0.164	0.113	0.247	0.180	0.201	0.239	0.190	0.185
Tafeng	20	0.097	0.185	0.170	0.114	0.242	0.181	0.185	0.239	0.191	0.187
Tafeng	30	0.081	0.183	0.184	0.113	0.233	0.178	0.180	0.247	0.187	0.183
Sales	10	0.073	0.110	0.075	0.081	0.213	0.118	0.266	0.190	0.132	0.107
Sales	20	0.075	0.103	0.084	0.085	0.212	0.120	0.264	0.190	0.116	0.102
Sales	30	0.076	0.099	0.080	0.087	0.213	0.120	0.261	0.188	0.116	0.102

 Table 4: Ablation study of the proposed method. The test total errors are shown. ‘w/o-Net’ is without neural networks in the deep kernel GP, ‘w/o- r ’ is without calibration model r , ‘w/o- \mathcal{L}_C ’ is without calibration loss \mathcal{L}_C in the objective function in Eq. (11), ‘w/o-Mix’ is without the mixing of the uncalibrated CDF in Eq. (9) or fixing $\alpha = 1$, ‘w/-Split’ is with support set splitting for adaptation and calibration, and ‘w/- r_{emp} ’ uses the empirical calibration model in Eq. (2) for calibration. Values in bold typeface are not statistically significantly different at the 5% level from the best performing method in each row according to a paired t-test.

Data	N^S	Ours	w/o-Net	w/o- r	w/o- \mathcal{L}_C	w/o-Mix	w/-Split	w/- r_{emp}
AHM	10	0.167	0.185	0.176	0.195	0.167	0.255	0.172
AHM	20	0.097	0.103	0.115	0.138	0.099	0.160	0.102
AHM	30	0.077	0.078	0.094	0.122	0.077	0.116	0.083
MAT	10	0.123	0.136	0.133	0.149	0.126	0.165	0.128
MAT	20	0.094	0.099	0.104	0.119	0.093	0.117	0.098
MAT	30	0.077	0.083	0.093	0.105	0.080	0.099	0.084
School	10	0.383	0.531	0.384	0.464	0.399	0.381	0.385
School	20	0.380	0.506	0.379	0.460	0.390	0.377	0.391
School	30	0.373	0.470	0.373	0.453	0.379	0.374	0.383
Tafeng	10	0.957	1.159	0.882	0.961	0.875	0.939	0.772
Tafeng	20	0.882	1.094	0.517	0.939	0.889	0.897	0.832
Tafeng	30	0.134	0.146	0.159	0.215	0.155	0.155	0.146
Sales	10	0.081	0.144	0.086	0.161	0.087	0.081	0.089
Sales	20	0.081	0.104	0.091	0.159	0.088	0.079	0.086
Sales	30	0.082	0.093	0.085	0.159	0.085	0.083	0.086

Table 4 shows the ablation study result. The better performance of the proposed method exhibits the effectiveness of each component. Since the neural networks are used for sharing knowledge across tasks, the proposed method without neural networks (w/o-Net) deteriorated the performance. The proposed method without calibration models (w/o- r) corresponds to MDKL that minimizes the expected test total error, which includes the expected test calibration error. The increased error of w/o- r shows the effectiveness of our calibration model for calibrating the output distribution. With the calibration loss, the expected test uncertainty estimation performance is directly optimized. Therefore, removing the calibration loss (w/o- \mathcal{L}_C) resulted in an increase of the total error. The results without the mixing of the uncalibrated CDF (w/o-Mix) and those with the support set splitting (w/-Split) indicate that mixing and unsplitting sometimes improve the performance. Since the empirical calibration model (w/- r_{emp}) is not differentiable, its performance was low. Figure 6 shows the test errors with different $\lambda \in \{10^{-2}, 0.1, 0.2, \dots, 1.0\}$. The test error was not sensitive to λ unless λ was close to zero or one.

We also compared with SQR, NG, BD, and GP methods that were trained using meta-training datasets: ASAR, ANG, ABD, and AGP. In AGP, sparse GPs [58] were used with task-shared pseudo-inputs and task-specific support instances.

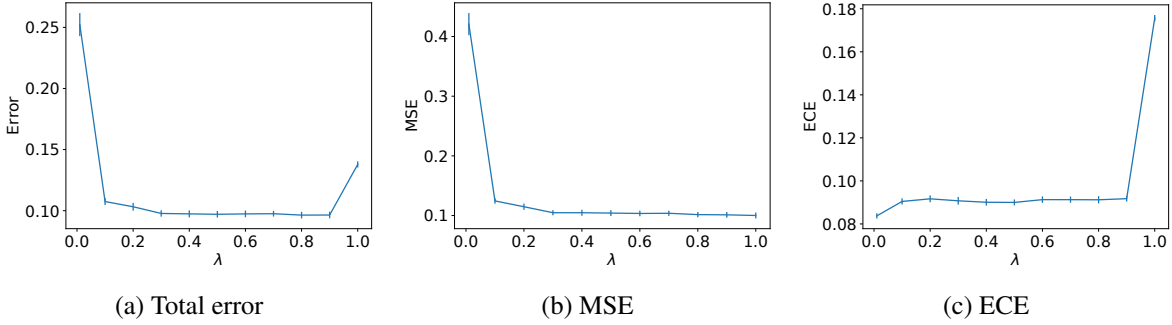


Figure 6: Test total error (a), MSE (b), and ECE (c) with different hyperparameters λ with the AHM datasets. The bar shows the standard error.

Table 5: Test total error, which is the average of MSE and ECE, with different numbers of support instances N^S . Values in bold typeface are not statistically significantly different at the 5% level from the best performing method in each row according to a paired t-test.

Data	N^S	Ours	ASQR	ANG	ABD	AGP
AHM	10	0.167	0.834	0.885	0.890	0.278
AHM	20	0.097	0.824	0.876	0.883	0.189
AHM	30	0.077	0.817	0.862	0.873	0.158
MAT	10	0.123	0.272	0.385	0.325	0.131
MAT	20	0.094	0.271	0.385	0.326	0.115
MAT	30	0.077	0.277	0.386	0.328	0.106
School	10	0.383	0.390	0.417	0.474	0.429
School	20	0.380	0.386	0.409	0.468	0.425
School	30	0.373	0.381	0.404	0.465	0.421
Tafeng	10	0.957	0.911	1.081	0.769	1.136
Tafeng	20	0.882	0.828	1.060	0.975	1.123
Tafeng	30	0.134	0.145	0.266	0.208	0.190
Sales	10	0.081	0.084	0.282	0.121	0.133
Sales	20	0.081	0.082	0.275	0.110	0.133
Sales	30	0.082	0.085	0.278	0.121	0.136

Table 6: Computational time in seconds for meta-learning on the AHM dataset with 20 support instances.

Ours	MDKL	NP	MSQR	MNG	MBD
588.745	264.324	83.448	4310.218	312.226	548.077

Table 7: Computational time in seconds for inference on the AHM dataset with 20 support instances.

Ours	MDKL	NP	MSQR	MNG	MBD	SQR	NG	BD	GP
0.083	0.034	0.015	0.316	0.047	0.112	5.853	5.677	51.407	0.020

Table 5 shows their test total error. When appropriate regression models are different across tasks, these methods did not perform well. The proposed method achieved the lowest test total error in all cases.

Table 6 shows the computational time in seconds for meta-learning using computers with Xeon Gold 6130 2.10GHz CPU, and 256GB memory. Table 7 shows the time in seconds to output predicted target values and CDFs that are adapted and calibrated to the support set. Although the proposed method requires a long meta-learning time, its inference time is short.

6 Conclusion

We proposed a meta-learning method for regression uncertainty estimation, and confirmed that the proposed method achieves better performance than the existing methods. For future work, we plan to consider individual calibration

instead of average calibration [11] to approximate the conditional quantiles. Also, we would like to extend the proposed method for classification tasks.

References

- [1] M. Abdar, F. Pourpanah, S. Hussain, D. Rezazadegan, L. Liu, M. Ghavamzadeh, P. Fieguth, X. Cao, A. Khosravi, U. R. Acharya, et al. A review of uncertainty quantification in deep learning: Techniques, applications and challenges. *Information Fusion*, 76:243–297, 2021.
- [2] A. Argyriou, T. Evgeniou, and M. Pontil. Multi-task feature learning. *Advances in Neural Information Processing Systems*, 2006.
- [3] B. Bakker and T. Heskes. Task clustering and gating for Bayesian multitask learning. *Journal of Machine Learning Research*, 4:83–99, 2003.
- [4] E. Begoli, T. Bhattacharya, and D. Kusnezov. The need for uncertainty quantification in machine-assisted medical decision making. *Nature Machine Intelligence*, 1(1):20–23, 2019.
- [5] Y. Bengio, S. Bengio, and J. Cloutier. Learning a synaptic learning rule. In *International Joint Conference on Neural Networks*, 1991.
- [6] L. Bertinetto, J. F. Henriques, P. Torr, and A. Vedaldi. Meta-learning with differentiable closed-form solvers. In *International Conference on Learning Representations*, 2018.
- [7] C. Blundell, J. Cornebise, K. Kavukcuoglu, and D. Wierstra. Weight uncertainty in neural network. In *International Conference on Machine Learning*, pages 1613–1622, 2015.
- [8] O. Bohdal, Y. Yang, and T. Hospedales. Meta-calibration: Meta-learning of model calibration using differentiable expected calibration error. *arXiv preprint arXiv:2106.09613*, 2021.
- [9] K. Chua, R. Calandra, R. McAllister, and S. Levine. Deep reinforcement learning in a handful of trials using probabilistic dynamics models. *Advances in Neural Information Processing Systems*, 31, 2018.
- [10] Y. Chung, I. Char, H. Guo, J. Schneider, and W. Neiswanger. Uncertainty toolbox: an open-source library for assessing, visualizing, and improving uncertainty quantification. *arXiv preprint arXiv:2109.10254*, 2021.
- [11] Y. Chung, W. Neiswanger, I. Char, and J. Schneider. Beyond pinball loss: Quantile methods for calibrated uncertainty quantification. *Advances in Neural Information Processing Systems*, 34:10971–10984, 2021.
- [12] P. Cui, W. Hu, and J. Zhu. Calibrated reliable regression using maximum mean discrepancy. *Advances in Neural Information Processing Systems*, 33:17164–17175, 2020.
- [13] A. P. Dawid. The well-calibrated Bayesian. *Journal of the American Statistical Association*, 77(379):605–610, 1982.
- [14] M. Fasiolo, S. N. Wood, M. Zaffran, R. Nedellec, and Y. Goude. Fast calibrated additive quantile regression. *Journal of the American Statistical Association*, 116(535):1402–1412, 2021.
- [15] C. Finn, P. Abbeel, and S. Levine. Model-agnostic meta-learning for fast adaptation of deep networks. In *International conference on machine learning*, pages 1126–1135, 2017.
- [16] V. Fortuin, H. Strathmann, and G. Rätsch. Meta-learning mean functions for Gaussian processes. *arXiv preprint arXiv:1901.08098*, 2019.
- [17] F. Futami, T. Iwata, I. Sato, M. Sugiyama, et al. Loss function based second-order jensen inequality and its application to particle variational inference. *Advances in Neural Information Processing Systems*, 34:6803–6815, 2021.
- [18] Y. Gal and Z. Ghahramani. Dropout as a Bayesian approximation: Representing model uncertainty in deep learning. In *International Conference on Machine Learning*, pages 1050–1059, 2016.
- [19] Y. Gal, R. Islam, and Z. Ghahramani. Deep Bayesian active learning with image data. In *International Conference on Machine Learning*, pages 1183–1192, 2017.
- [20] J. Garcia and F. Fernández. Safe exploration of state and action spaces in reinforcement learning. *Journal of Artificial Intelligence Research*, 45:515–564, 2012.
- [21] M. Garnelo, D. Rosenbaum, C. Maddison, T. Ramalho, D. Saxton, M. Shanahan, Y. W. Teh, D. Rezende, and S. A. Eslami. Conditional neural processes. In *International Conference on Machine Learning*, pages 1704–1713, 2018.
- [22] M. Garnelo, J. Schwarz, D. Rosenbaum, F. Viola, D. J. Rezende, S. Eslami, and Y. W. Teh. Neural processes. *arXiv preprint arXiv:1807.01622*, 2018.

- [23] T. Gneiting and A. E. Raftery. Strictly proper scoring rules, prediction, and estimation. *Journal of the American statistical Association*, 102(477):359–378, 2007.
- [24] C. Guo, G. Pleiss, Y. Sun, and K. Q. Weinberger. On calibration of modern neural networks. In *International Conference on Machine Learning*, pages 1321–1330, 2017.
- [25] J. Harrison, A. Sharma, and M. Pavone. Meta-learning priors for efficient online Bayesian regression. In *Algorithmic Foundations of Robotics XIII: Proceedings of the 13th Workshop on the Algorithmic Foundations of Robotics 13*, pages 318–337. Springer, 2020.
- [26] X. He, F. Alesiani, and A. Shaker. Efficient and scalable multi-task regression on massive number of tasks. In *Proceedings of the AAAI Conference on Artificial Intelligence*, volume 33, pages 3763–3770, 2019.
- [27] J. M. Hernández-Lobato and R. Adams. Probabilistic backpropagation for scalable learning of Bayesian neural networks. In *International Conference on Machine Learning*, pages 1861–1869, 2015.
- [28] T. Iwata and Y. Tanaka. Few-shot learning for spatial regression via neural embedding-based Gaussian processes. *Machine Learning*, 111:1239–1257, 2022.
- [29] S. Jeon, C. J. Paciorek, and M. F. Wehner. Quantile-based bias correction and uncertainty quantification of extreme event attribution statements. *Weather and Climate Extremes*, 12:24–32, 2016.
- [30] D. Y. Kang, P. N. DeYoung, J. Tantiogloc, T. P. Coleman, and R. L. Owens. Statistical uncertainty quantification to augment clinical decision support: a first implementation in sleep medicine. *NPJ Digital Medicine*, 4(1):1–9, 2021.
- [31] H. Kim, A. Mnih, J. Schwarz, M. Garnelo, A. Eslami, D. Rosenbaum, O. Vinyals, and Y. W. Teh. Attentive neural processes. In *International Conference on Learning Representations*, 2018.
- [32] S. Kim and S.-Y. Yun. Calibration of few-shot classification tasks: Mitigating misconfidence from distribution mismatch. *IEEE Access*, 10:53894–53908, 2022.
- [33] D. P. Kingma and J. Ba. Adam: A method for stochastic optimization. In *International Conference on Learning Representations*, 2015.
- [34] D. Koller and N. Friedman. *Probabilistic graphical models: principles and techniques*. MIT press, 2009.
- [35] V. Kuleshov, N. Fenner, and S. Ermon. Accurate uncertainties for deep learning using calibrated regression. In *International Conference on Machine Learning*, pages 2796–2804, 2018.
- [36] A. Kumar, S. Sarawagi, and U. Jain. Trainable calibration measures for neural networks from kernel mean embeddings. In *International Conference on Machine Learning*, pages 2805–2814, 2018.
- [37] B. Lakshminarayanan, A. Pritzel, and C. Blundell. Simple and scalable predictive uncertainty estimation using deep ensembles. *Advances in Neural Information Processing Systems*, 30, 2017.
- [38] W. J. Maddox, P. Izmailov, T. Garipov, D. P. Vetrov, and A. G. Wilson. A simple baseline for Bayesian uncertainty in deep learning. *Advances in Neural Information Processing Systems*, 32, 2019.
- [39] A. Malik, V. Kuleshov, J. Song, D. Nemer, H. Seymour, and S. Ermon. Calibrated model-based deep reinforcement learning. In *International Conference on Machine Learning*, pages 4314–4323, 2019.
- [40] C. Marx, S. Zhao, W. Neiswanger, and S. Ermon. Modular conformal calibration. In *International Conference on Machine Learning*, pages 15180–15195, 2022.
- [41] R. Michelmoro, M. Wicker, L. Laurenti, L. Cardelli, Y. Gal, and M. Kwiatkowska. Uncertainty quantification with statistical guarantees in end-to-end autonomous driving control. In *IEEE International Conference on Robotics and Automation*, pages 7344–7350, 2020.
- [42] M. P. Naeini, G. Cooper, and M. Hauskrecht. Obtaining well calibrated probabilities using Bayesian binning. In *Twenty-Ninth AAAI Conference on Artificial Intelligence*, 2015.
- [43] T. Nguyen and A. Grover. Transformer neural processes: Uncertainty-aware meta learning via sequence modeling. *arXiv preprint arXiv:2207.04179*, 2022.
- [44] A. Niculescu-Mizil and R. Caruana. Predicting good probabilities with supervised learning. In *International Conference on Machine Learning*, pages 625–632, 2005.
- [45] A. Paszke, S. Gross, F. Massa, A. Lerer, J. Bradbury, G. Chanan, T. Killeen, Z. Lin, N. Gimelshein, L. Antiga, et al. Pytorch: An imperative style, high-performance deep learning library. *Advances in Neural Information Processing Systems*, 32, 2019.
- [46] M. Patacchiola, J. Turner, E. J. Crowley, M. O’Boyle, and A. J. Storkey. Bayesian meta-learning for the few-shot setting via deep kernels. *Advances in Neural Information Processing Systems*, 33:16108–16118, 2020.

- [47] T. Pearce, A. Brintrup, M. Zaki, and A. Neely. High-quality prediction intervals for deep learning: A distribution-free, ensembled approach. In *International Conference on Machine Learning*, pages 4075–4084, 2018.
- [48] J. Platt. Probabilistic outputs for support vector machines and comparisons to regularized likelihood methods. *Advances in Large Margin Classifiers*, 10(3):61–74, 1999.
- [49] C. E. Rasmussen and C. K. I. Williams. *Gaussian Processes for Machine Learning*. The MIT Press, 2005.
- [50] S. Ravi and H. Larochelle. Optimization as a model for few-shot learning. In *International Conference on Learning Representations*, 2017.
- [51] J. Rothfuss, D. Heyn, A. Krause, et al. Meta-learning reliable priors in the function space. *Advances in Neural Information Processing Systems*, 34:280–293, 2021.
- [52] R. Sahoo, S. Zhao, A. Chen, and S. Ermon. Reliable decisions with threshold calibration. *Advances in Neural Information Processing Systems*, 34:1831–1844, 2021.
- [53] T. S. Salem, H. Langseth, and H. Ramampiaro. Prediction intervals: Split normal mixture from quality-driven deep ensembles. In *Conference on Uncertainty in Artificial Intelligence*, pages 1179–1187, 2020.
- [54] J. Schmidhuber. Evolutionary principles in self-referential learning. on learning now to learn: The meta-meta-meta...-hook. Master’s thesis, Technische Universitat Munchen, Germany, 1987.
- [55] B. Shahriari, K. Swersky, Z. Wang, R. P. Adams, and N. De Freitas. Taking the human out of the loop: A review of Bayesian optimization. *Proceedings of the IEEE*, 104(1):148–175, 2015.
- [56] N. Skafta, M. Jørgensen, and S. Hauberg. Reliable training and estimation of variance networks. *Advances in Neural Information Processing Systems*, 32, 2019.
- [57] J. Snell, K. Swersky, and R. Zemel. Prototypical networks for few-shot learning. *Advances in Neural Information Processing Systems*, 30, 2017.
- [58] E. Snelson and Z. Ghahramani. Sparse Gaussian processes using pseudo-inputs. *Advances in Neural Information Processing Systems*, 18, 2005.
- [59] H. Song, T. Diethe, M. Kull, and P. Flach. Distribution calibration for regression. In *International Conference on Machine Learning*, pages 5897–5906, 2019.
- [60] N. Tagasovska and D. Lopez-Paz. Single-model uncertainties for deep learning. *Advances in Neural Information Processing Systems*, 32, 2019.
- [61] S. C. Tan and J. P. S. Lau. Time series clustering: A superior alternative for market basket analysis. In *Proceedings of International Conference on Advanced Data and Information Engineering*, pages 241–248. Springer, 2014.
- [62] P. Tossou, B. Dura, F. Laviolette, M. Marchand, and A. Lacoste. Adaptive deep kernel learning. *arXiv preprint arXiv:1905.12131*, 2019.
- [63] G.-L. Tran, E. V. Bonilla, J. Cunningham, P. Michiardi, and M. Filippone. Calibrating deep convolutional Gaussian processes. In *The 22nd International Conference on Artificial Intelligence and Statistics*, pages 1554–1563, 2019.
- [64] O. Vinyals, C. Blundell, T. Lillicrap, D. Wierstra, et al. Matching networks for one shot learning. In *Advances in Neural Information Processing Systems*, pages 3630–3638, 2016.
- [65] V. Vovk, I. Petej, P. Toccaceli, A. Gammerman, E. Ahlberg, and L. Carlsson. Conformal calibrators. In *Conformal and Probabilistic Prediction and Applications*, pages 84–99, 2020.
- [66] A. G. Wilson, Z. Hu, R. Salakhutdinov, and E. P. Xing. Deep kernel learning. In *International Conference on Artificial Intelligence and Statistics*, pages 370–378, 2016.
- [67] P. Yang, S. Ren, Y. Zhao, and P. Li. Calibrating cnns for few-shot meta learning. In *Proceedings of the IEEE/CVF Winter Conference on Applications of Computer Vision*, pages 2090–2099, 2022.
- [68] T. Yu, G. Thomas, L. Yu, S. Ermon, J. Y. Zou, S. Levine, C. Finn, and T. Ma. MOPO: Model-based offline policy optimization. *Advances in Neural Information Processing Systems*, 33:14129–14142, 2020.
- [69] S. Zhao, T. Ma, and S. Ermon. Individual calibration with randomized forecasting. In *International Conference on Machine Learning*, pages 11387–11397, 2020.